

# Frequency and voltage dependence of the electrical and dielectric properties of Au/n-Si Schottky diodes with SiO<sub>2</sub> insulator layer

A. TATAROĞLU

*Physics Department, Faculty of Arts and Sciences, Gazi University, 06500, Teknikokullar, Ankara, Turkey*

In this paper, the frequency and voltage dependence of the electrical and dielectric properties of metal-insulator-semiconductor (MIS) Schottky diodes has been investigated using capacitance-voltage (C-V) and conductance-voltage (G/ω-V) characteristics in the frequency range of 1 kHz-1 MHz at room temperature. Calculations of the dielectric constant ( $\epsilon'$ ), dielectric loss ( $\epsilon''$ ), loss tangent ( $\tan\delta$ ), ac conductivity ( $\sigma_{ac}$ ), ac resistivity ( $\rho_{ac}$ ) and the electric modulus are given in the studied frequency ranges. Experimental results show that the values of the dielectric parameters are strongly dependent on frequency and voltage. The values of  $\epsilon'$  and  $\epsilon''$  decreased with the increasing frequency, while those of  $\sigma_{ac}$  increased with the increasing frequency. Also, electric modulus formalism has been analyzed to obtain the experimental dielectric data. The results imply that the interfacial polarization can occur more easily at low frequencies and consequently contribute to the deviation of dielectric properties of MIS Schottky diodes.

(Received June 3, 2011; accepted August 10, 2011)

*Keywords:* MIS Schottky diodes; C-V and G/ω-V characteristics; Dielectric properties; ac conductivity; ac resistivity; Electric modulus

## 1. Introduction

Semiconductor devices are the basic components of integrated circuits and are responsible for the startling rapid growth of electronics industry. Because there is a continuing need for faster and more complex systems for the information age, existing semiconductor devices are being studied for improvement, and new ones are being invented [1-3]. The semiconductor devices such as metal-semiconductor (MS) diodes, metal-insulator-semiconductor(MIS)-type Schottky diodes and metal-oxide-semiconductor (MOS) capacitors have an important role in modern electronics, and MS diodes are one of the most widely used rectifying contacts in the electronics industry [1,4,5]. In MIS and MOS structures, metal and semiconductor remain separated by an interfacial insulator layer such as SiO<sub>2</sub>, SnO<sub>2</sub>, Si<sub>3</sub>N<sub>4</sub>, TiO<sub>2</sub> and at metal/semiconductor. There is a continuous distribution of surface states with energies located in the band gap of semiconductor. The performance and reliability of these devices depend especially on the formation of the interfacial insulator layer, interface states ( $N_{ss}$ ) localized at the semiconductor/insulator interface and the series resistance ( $R_s$ ) [6,7].

The interfacial insulator layer, interface state and series resistance values cause the electrical characteristics of MIS structures to be non-ideal [8-10]. Also, the change in bias voltage and frequency has important effects on the electrical and dielectric parameters of these structures [11-16]. When a voltage is applied across the MIS structure, the combination of the interfacial insulator layer, depletion layer and the series resistance of the device will share the applied voltage.

This paper presents a detailed study on the electrical and dielectric properties in the frequency range of 1 kHz-1 MHz at room temperature for Au/SiO<sub>2</sub>/n-Si (MIS) Schottky diodes. The admittance technique was used to determine the dielectric constant ( $\epsilon'$ ), dielectric loss ( $\epsilon''$ ), loss tangent ( $\tan\delta$ ), ac conductivity ( $\sigma_{ac}$ ), ac resistivity ( $\rho_{ac}$ ) and the electric modulus of MIS Schottky diodes [5,14].

## 2. Experimental detail

Au/SiO<sub>2</sub>/n-Si (MIS) Schottky diodes used in this study have been prepared using cleaned and polished as received from manufacturer n-type (P-doped) single crystals silicon wafer with (100) surface orientation, 300 μm thick, 2" diameter and 0.5 Ω.cm resistivity. Before making contacts, the n-Si wafer was degreased in organic solvent of CHCl<sub>3</sub>, CH<sub>3</sub>COCH and CH<sub>3</sub>OH consecutively and then etched in a sequence of H<sub>2</sub>SO<sub>4</sub> an H<sub>2</sub>O<sub>2</sub>, 20% HF, a solution of 6HNO<sub>3</sub>: 1 HF: 35 H<sub>2</sub>O, 20% HF and finally quenched in de-ionised water for a prolonged time. Preceding each cleaning step, the wafer was rinsed thoroughly in de-ionized water of resistivity of 18 MΩ-cm. After surface cleaning, the ohmic and rectifier contacts were formed using thermal evaporation system. The ohmic back contacts were formed by deposition of high purity Au (99.999%) with ~2000 Å thickness at 450 °C, under ~1x10<sup>-6</sup> Torr vacuum and the sample was annealed at 400 °C to achieve good ohmic contact behavior. The oxidations are carried out in a resistance-heated furnace in dry oxygen with a flow rate of a 1.5 l/min and the insulator layer thickness is grown at the temperatures of 650 °C during 1.5 h. After then, dot shaped rectifier front contacts with 1 mm diameter and

~2000 Å thickness were formed by deposition of high purity Au (99.999%) at 70 °C. The interfacial insulator layer thickness was estimated to be about 30 Å from high frequency (1 MHz) measurement of the interface insulator capacitance in the strong accumulation region for Au/SiO<sub>2</sub>/n-Si (MIS) Schottky diodes.

The capacitance-voltage (C-V) and conductance-voltage (G/ω-V) measurements were performed in the frequency range of 1 kHz-1 MHz at room temperature by using a HP 4192A HF/LF impedance analyzer (5 Hz-13 MHz) working in parallel circuit mode. The ac signal amplitude was kept at 50 mV. Furthermore, all measurements were carried out with the help of a microcomputer through an IEEE-488 ac/dc converter card.

### 3. Results and discussion

#### 3.1. Frequency and bias voltage dependence of C and G/ω

The capacitance-voltage (C-V) and conductance-voltage (G/ω-V) measurements under reverse and forward bias were performed over a frequency range of 1 kHz-1 MHz at room temperature. Fig. 1(a) and (b) show the capacitance (C) and conductance (G/ω) as a function of frequency in the voltage range of 0-1 V with steps of 0.25 V. As can be seen in Fig. 1(a) and (b), the measured C and G/ω has displayed an decreasing trend with increasing frequency in the frequency range of 1 kHz-1 MHz. Such behavior of the capacitance and conductance is attributed to particular distribution of interface states (N<sub>ss</sub>) between metal-semiconductor [15-21]. Also, this behavior is attributed to the presence of a continuous distribution of N<sub>ss</sub>, which leads to a progressive decrease of the response of the N<sub>ss</sub> to the applied alternating-current voltage [17,19,21-26]. At low frequencies, the N<sub>ss</sub> can easily follow the ac signal and yield an excess capacitance, which depends on the frequency and time constant of interface states. However, in the sufficiently high frequency limit (f ≥ 500 kHz), the N<sub>ss</sub> can hardly follow the ac signal and the contribution of interface states capacitance to the total capacitance may be neglected. Also, the series resistance (R<sub>s</sub>) causes a serious error in the extraction of electrical and dielectric parameters of MIS/MOS structures from the C-V and G/ω-V measurements. Similar behavior was observed in the literature [4,6,15,19,21,23-25].

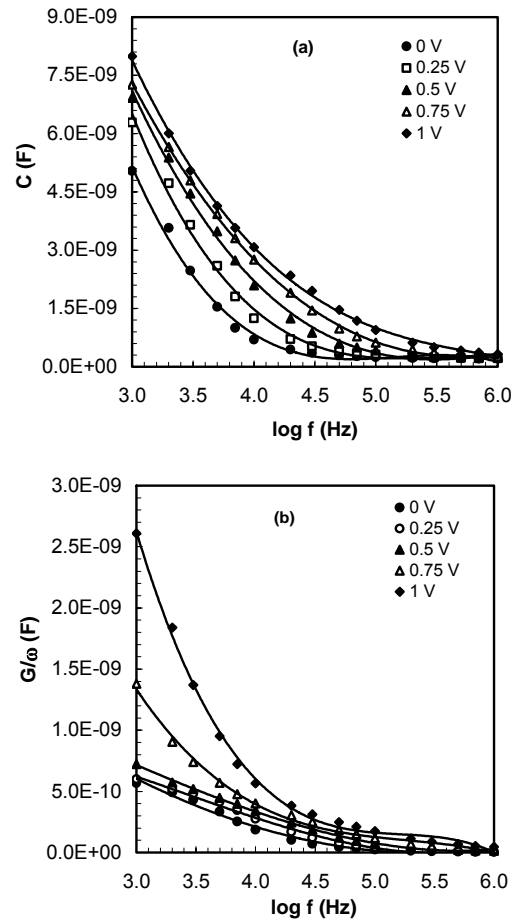


Fig. 1. The frequency dependence of (a) the  $C(V_C)$ - $\log f$  and (b)  $G/\omega(V_C)$ - $\log f$  characteristics of MIS Schottky diode for various forward bias voltages at room temperature.

#### 3.2. Frequency and voltage dependence of dielectric properties

In this section, frequency and voltage dependence of dielectric constant ( $\epsilon'$ ), dielectric loss ( $\epsilon''$ ), loss tangent ( $\tan\delta$ ), ac conductivity ( $\sigma_{ac}$ ), ac resistivity ( $\rho_{ac}$ ) and the real and imaginary parts of the electric modulus ( $M'$  and  $M''$ ) are studied for Au/SiO<sub>2</sub>/n-Si (MIS) Schottky diode. At room temperature, the values of the dielectric properties measured as a function of frequency in the 1 kHz to 1 MHz range.

The complex permittivity can be defined in the following complex form [27,28],

$$\varepsilon^*(\omega) = \varepsilon'(\omega) - j\varepsilon''(\omega) \quad (1)$$

where  $\varepsilon'$  and  $\varepsilon''$  are the real and the imaginary parts of complex permittivity, and  $j$  is the root of -1. The real part of the permittivity,  $\varepsilon'(\omega)$ , is a measure of the energy stored from the applied electric field in the material and identifies the strength of alignment of dipoles in the dielectric. The imaginary part,  $\varepsilon''(\omega)$ , or loss factor, is the energy dissipated in the dielectric associated with the frictional dampening that prevent displacements of bound charge from remaining in phase with the field changes [29].

The complex permittivity formalism has been employed to describe the electrical and dielectric properties. In the  $\varepsilon^*$  formalism, in the case of admittance measurements, the following relation holds

$$\varepsilon^* = \frac{Y^*}{j\omega C_o} = \frac{C}{C_o} - j\frac{G}{\omega C_o} \quad (2)$$

where  $Y^*$ ,  $C$  and  $G$  are the measured admittance, capacitance and conductance values of the dielectric material, respectively, and  $\omega$  is the angular frequency ( $\omega=2\pi f$ ) of the applied electric field [30].

The real part of the complex permittivity, the dielectric constant ( $\varepsilon'$ ), at the various frequencies is calculated using the measured capacitance values at the strong accumulation region from the relation [31,32]

$$\varepsilon'(\omega) = \frac{C_m}{C_o} \quad (3)$$

where  $C_o$  is capacitance of an empty capacitor.  $C_o = \varepsilon_o(A/d)$ ; where  $A$  is the rectifier contact area in  $\text{cm}^2$ ,  $d$  is the interfacial insulator layer thickness and  $\varepsilon_o$  is the permittivity of free space charge ( $\varepsilon_o = 8.85 \times 10^{-14}$  F/cm), and  $C_m$  is measurement maximal capacitance of MIS structure in the strong accumulation region, correspond to the oxide capacitance.

The imaginary part of the complex permittivity, the dielectric loss ( $\varepsilon''$ ), at the various frequencies is calculated using the measured conductance values from the relation

$$\varepsilon''(\omega) = \frac{G_m}{\omega C_o} \quad (4)$$

The dissipation factor or loss tangent ( $\tan\delta$ ) can be expressed as follows [27,28,31-33],

$$\tan \delta = \frac{\varepsilon''(\omega)}{\varepsilon'(\omega)} \quad (5)$$

The ac conductivity of all samples has been calculated from the dielectric losses according to the relation

$$\sigma^* = i\varepsilon_o\omega\varepsilon^*(\omega) = \varepsilon_o\omega\varepsilon'' + i\varepsilon_o\omega\varepsilon' \quad (6)$$

The real part of  $\sigma^*(\omega)$  is given by

$$\sigma_{ac} = \omega C \tan \delta (d/A) = \varepsilon_o \omega \varepsilon'' \quad (7)$$

As it turns out the effect of conductivity can be highly suppressed when the data are presented in the modulus representation. The electric modulus approach began when the reciprocal complex permittivity was discussed as an electrical analogue to the mechanical shear modulus [30]. From the physical point of view, the electrical modulus corresponds to the relaxation of the electric field in the material when the electric displacement remains constant. Therefore, the modulus represents the real dielectric relaxation process [34,35]. The complex modulus  $M^*(\omega)$  was introduced to describe the dielectric response of non-conducting materials. This formalism has been applied also to materials with non-zero conductivity. The starting point for further consideration is the definition of the dielectric modulus: [30,36].

$$M^*(\omega) = \frac{1}{\varepsilon^*} = M'(\omega) + iM''(\omega) \quad (8)$$

$$M'(\omega) = \frac{\varepsilon'(\omega)}{\varepsilon'(\omega)^2 + \varepsilon''(\omega)^2}$$

and

$$M''(\omega) = \frac{\varepsilon''(\omega)}{\varepsilon'(\omega)^2 + \varepsilon''(\omega)^2} \quad (9)$$

where  $M'$  and  $M''$  are the real and the imaginary parts of complex modulus. Based on Eq. (11) we have changed the form of presentation of the dielectric data from  $\varepsilon'(\omega)$  and  $\varepsilon''(\omega)$  to  $M'(\omega)$  and  $M''(\omega)$ .

Fig. 2(a), (b) and (c) show the frequency-dependent  $\varepsilon'$ ,  $\varepsilon''$  and  $\tan\delta$  curves of MIS Schottky diode for various forward bias voltages at room temperature. As seen in Fig. 2, changes in the frequency and applied bias voltage considerably affect  $\varepsilon'$ ,  $\varepsilon''$  and  $\tan\delta$  values. As can be seen from these figures, the values of  $\varepsilon'$  and  $\varepsilon''$  decrease with an increase in frequency for each voltage. This is the normal behavior of a dielectric material. In principle, at low frequencies, all the four types of polarization processes, i.e., the electronic, ionic, dipolar, and interfacial or surface polarization contribute to the values of  $\varepsilon'$  and  $\varepsilon''$ . With increasing frequency, the contributions of the interfacial, dipolar or the ionic polarization become ineffective by leaving behind only the electronic part. Furthermore, the decrease in  $\varepsilon'$  and  $\varepsilon''$  with an increase in frequency is explained by the fact that as the frequency is raised, the interfacial dipoles have less time to orient themselves in the direction of the alternating field [23,24,37-42]. On the other hand, after 100 kHz, the change in dielectric properties ( $\varepsilon'$  and  $\varepsilon''$ ) continues to decrease slightly, and also remains almost constant at higher frequencies (100 kHz-1 MHz), with the increasing frequency. This behavior in dielectric properties of MIS structures at the high

frequencies may be due to the interface states that cannot follow the ac signal at high frequency [12,33,43,44].

If the electric polarization in a dielectric is unable to follow the varying electric field, dielectric loss occurs. An applied field will alter this energy difference by producing a net polarization, which lags behind the applied field because the tunneling transition rates are finite. This part

of the polarization, which is not in phase with the applied field, is termed as dielectric loss. Fig. 2(c) shows the variation of the loss tangent ( $\tan\delta$ ) with frequency for each voltage. As shown in Fig. 2(c), the peak values of  $\tan\delta$ - $\log f$  decreased with the increasing voltage and the peak positions tend to shift towards high frequency region.

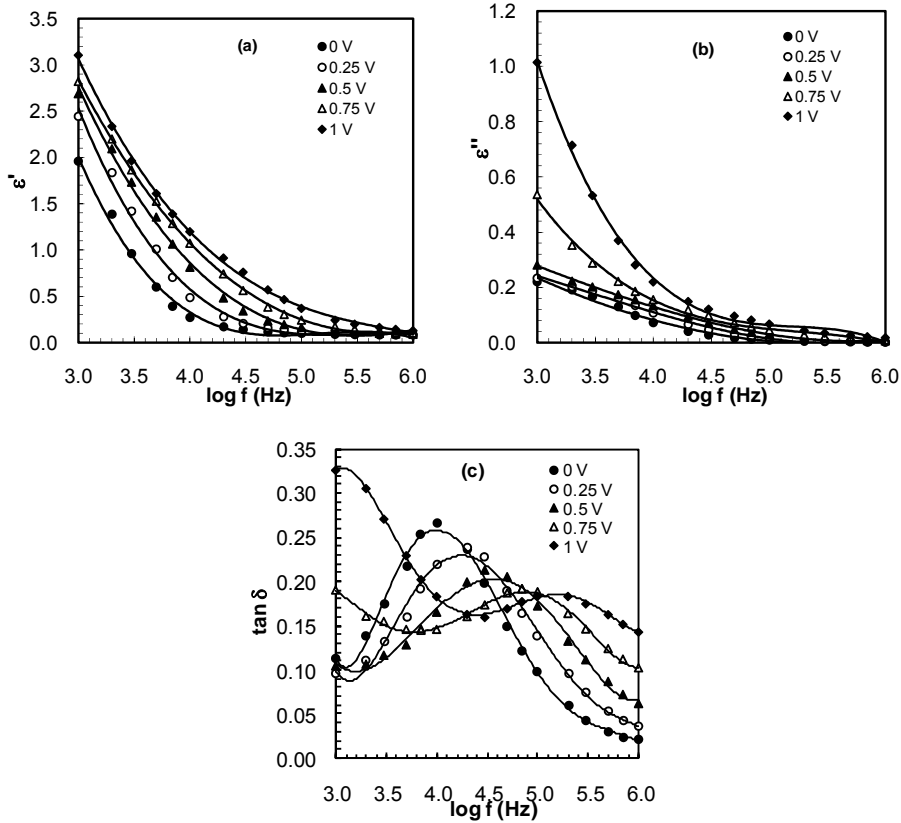


Fig. 2. Frequency dependence of the (a)  $\epsilon'$ , (b)  $\epsilon''$  and (c)  $\tan\delta$  of MIS Schottky diodes for various applied voltage.

Fig. 3 shows the frequency-dependent ac conductivity ( $\sigma_{ac}$ ) of MIS Schottky diode at various voltages. As can be seen in Fig. 3, ac conductivity increases with the increasing frequency. As seen in Eq. (6),  $\sigma_{ac}$  depends merely on the dielectric loss. As observed in Fig. 2(b) and 3, dielectric loss decreases with the increasing frequency and, accordingly,  $\sigma_{ac}$  increases. This result is also compatible with the literature, where it is suggested that the increase in ac conductivity with the increasing frequency is attributed to the series resistance effect. Similar behavior was observed in the literature [23,33,37-39,41,45-47].

Fig. 4 shows the variation of ac resistivity ( $\rho_{ac}$ ) with log frequency. The values of  $\rho_{ac}$  decrease with an increase in frequency from 1 kHz to 1 MHz. The increase in frequency of the applied field enhances the hopping of charge carriers resulting in an increase of conductivity and a decrease of resistivity. At higher frequencies ac resistivity decreases and remains constant because of the fact that hopping frequency can no longer follow the frequency of the applied external field leading to lower values of ac resistivity [34,48].

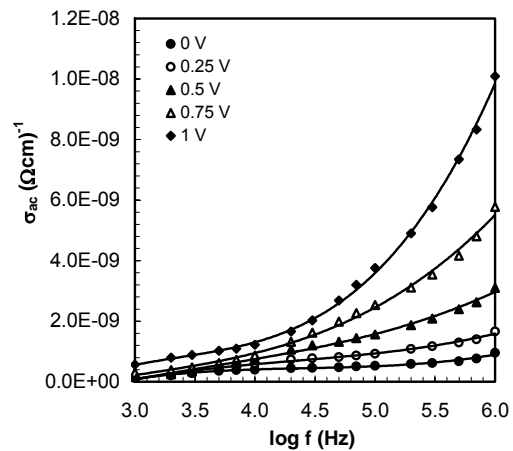


Fig. 3. Frequency dependence of ac conductivity ( $\sigma_{ac}$ ) of MIS Schottky diode for various applied voltage.

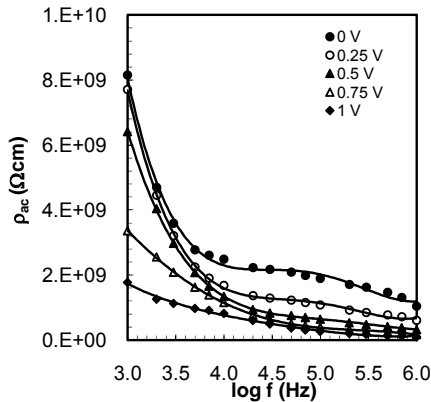


Fig. 4. Frequency dependence of ac resistivity ( $\rho_{ac}$ ) of MIS Schottky diode for various applied voltage.

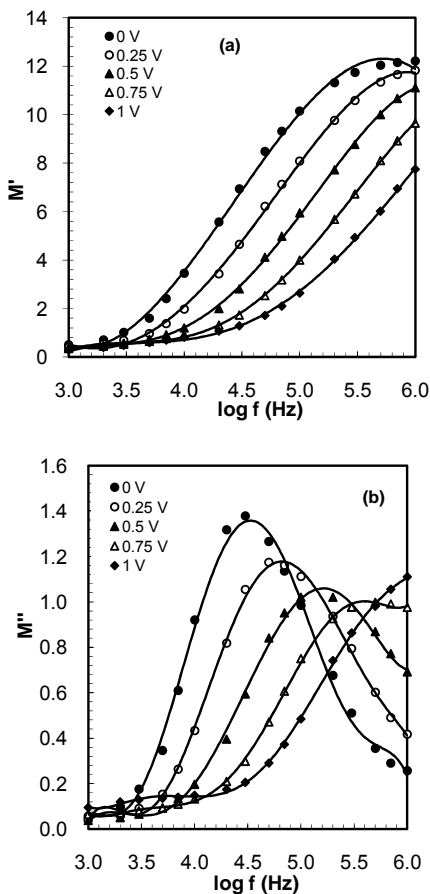


Fig. 5. (a) The real part  $M'$  and (b) the imaginary part  $M''$  of electric modulus  $M^*$  versus frequency for MIS Schottky diodes.

Fig. 5(a) and (b) show the frequency-dependent real ( $M'$ ) and imaginary ( $M''$ ) components of the electric modulus of MIS Schottky diode at various voltages. As seen in Fig. 5(a), the  $M'$  increases with the increasing frequency. As seen in Fig. 5(b), the  $M''$  has a peak for each

the voltage between  $\approx 10$  kHz and 300 kHz. The position of peak shifts to higher frequency with the increasing gate voltage. Similar studies have been reported in literature [30,34,36,37,46-50].

#### 4. Conclusions

The frequency and voltage dependence of electrical and dielectric properties Au/SiO<sub>2</sub>/n-Si (MIS) Schottky diodes have been studied in detail in the frequency range of 1 kHz–1MHz at room temperature using capacitance-voltage (C-V) and conductance-voltage ( $G/\omega$ -V) characteristics. It was shown that the electrical properties of MIS Schottky diode are strongly dependent on frequency and bias voltage. Since the presence of the interfacial insulator layer, interface states, fixed surface charge and series resistance causes changes in the electrical and dielectric characteristics of MIS structures. The values of dielectric constant ( $\epsilon'$ ) and dielectric loss ( $\epsilon''$ ) decrease with the increasing frequency for each bias voltage. These behaviors are attributed to the decrease in polarization with the increasing frequency in the metal-semiconductor interface. The values of ac conductivity ( $\sigma_{ac}$ ) and real part of electric modulus ( $M'$ ) increase with the increasing frequency for each bias voltage. It is concluded that the values of dielectric parameters of MIS Schottky diode are strongly dependent on both the frequency and applied bias voltage.

#### References

- [1] S.M. Sze, S M and K. Ng. Kwog, Physics of Semiconductor Devices, 3rd ed. Wiley, New Jersey, 2007.
- [2] M.S. Tyagi, Introduction to Semiconductor materials and Devices, Wiley, New York, 1991.
- [3] K.K. Kwok., Complete Guide to Semiconductor Devices, McGraw-Hill, New York, 1995.
- [4] A. Hiraki, Surface Sci. Rep. **3**, 357 (1983).
- [5] E.H. Rhoderick, R.H. Williams, Metal-Semiconductor Contacts, 2nd ed., Clarendon, Oxford, 1988.
- [6] M. Ambrico, M. Losurdo, P. Capezzuto, G. Bruno, T. Ligonzo, L. Schiavulli, I. Farella, V. Augelli, Solid-State Electron. **49**, 413 (2005).
- [7] A. Tataroğlu, Ş. Altındal, J. Alloys Compd. **484**, 405(2009).
- [8] M.K. Hudait, S.B. Krupanidhi, Solid-State Electron. **44**, 1089 (2000).
- [9] U. Kelberlau, R. Kassing, Solid-State Electron. **22**, 37 (1979).
- [10] R. Castagne, A. Vapaille, Surf. Sci. **28**, 157 (1971)
- [11] E.H. Nicollian, J.R. Brews, MOS (Metal-Oxide-Semiconductor) Physics and Technology, John Wiley, New York, 1982.
- [12] A. Tataroğlu, Microelectron. Eng. **83**, 2551 (2006)
- [13] A. Tataroğlu, Ş. Altındal, Vacuum **82**, 1203 (2008)

- [14] E.H. Nicollian, A. Goetzberger, *Appl. Phys. Lett.* **7**, 216 (1965).
- [15] H. Uslu, Ş. Altındal, U. Aydemir, İ. Dökme, İ.M. Afandiyeva, *J. Alloys Compd.* **503**, 96 (2010).
- [16] M. Siad, A. Keffous, S. Mamma, Y. Belkacem, H. Menari, *Appl. Surf. Sci.* **236**, 366 (2004).
- [17] E.H. Nicollian, A. Goetzberger, *Bell. Syst. Tech. J.* **46**, 1055 (1967).
- [18] P.Cova, A. Singh, R.A. Masut, *J. Appl. Phys.* **82**, 5217 (1997).
- [19] Ş. Karataş, A. Türüt, *Microelectron. Reliability* **50**, 351 (2010).
- [20] J.H. Werner, *Metallization and Metal-Semiconductor Interface*, Plenum, New York, 1989.
- [21] P. Chattopadhyay, B. Raychaudhuri, *Solid-State Electron.* **36**, 605 (1993).
- [22] B. Tataroğlu, Ş. Altındal, A. Tataroğlu, *Microelectron. Eng.* **83**, 2021 (2006).
- [23] O. Pakma, N. Serin, T. Serin, Ş. Altındal, *J. Phys. D: Appl. Phys.* **41**, 215103 (2008).
- [24] Ş. Karataş, *J. Non-Crys. Solids* **354**, 3606 (2008).
- [25] S. Duman, B. Gürbulak, S. Doğan, A. Türüt, *Vacuum* **85**, 798 (2011).
- [26] B. Akkal, Z. Benamara, B. Gruzza, L. Bideux, N.B. Bouiadjra, *Mater. Sci. Eng. C* **21**, 291 (2002).
- [27] C.P. Symth, *Dielectric Behaviour and Structure*, McGraw-Hill, New York, 1955.
- [28] Vera V. Daniel, *Dielectric Relaxation*, Academic Press, London, 1967.
- [29] D. Cheng, *Field and Wave Electromagnetics*, 2nd Ed., Addison-Wesley, New York, 1989.
- [30] N.G. McCrum, B.E. Read, G. Williams, *Anelastic and Dielectric Effects in Polymeric Solids*, Wiley, New York, 1967.
- [31] M. Popescu, I. Bunget, *Physics of Solid Dielectrics*, Elsevier, Amsterdam, 1984.
- [32] A. Chelkowski, *Dielectric Physics*, Elsevier, Amsterdam, 1980.
- [33] A. Tataroğlu, Ş. Altındal, M.M. Bülbül, *Microelectron. Eng.* **81**, 140 (2005).
- [34] Moti Ram, S. Chakrabarti, *J. Alloys Compd.* **462**, 214 (2008).
- [35] P. Kumar, B.P. Singh, T.P. Sinha, N.K. Singh, *Physica B* **406**, 139 (2011).
- [36] M.B. Mohamed, H. Wang, H. Fuess, *J. Phys. D: Appl. Phys.* **43**, 455409 (2010).
- [37] S.P. Szu, C.Y. Lin, *Mater. Chem. Phys.* **82**, 295 (2003).
- [38] D. Maurya, J. Kumar, Shripal, *J. Phys. Chem. Solids*, **66**, 1614 (2005).
- [39] A.A. Sattar, S.A. Rahman, *Phys. Stat. Sol. (a)* **200**, 415 (2003).
- [40] P. Matheswaran, R. Sathyamoorthy, R. Saravanakumar, S. Velumani, *Mater. Sci. Eng. B* **174**, 269 (2010).
- [41] K. Kumar, S.C. Katyal, P. Sharma, N. Thakur, *J. Optoelectron. Adv. Mater.* **13**, 371 (2011).
- [42] A.S. Md. S. Rahman, M.H. Islam, C.A. Hogarth, *Int. J. Electronics* **62**, 167 (1987).
- [43] N. Singh, A. Agarwal, S. Sanghi, *Current Appl. Phys.* **11**, 783 (2011).
- [44] Z. Jiwei, Y. Xi, W. Mingzhong, Z. Liangying, *J. Phys. D* **34** (2001) 1413.
- [45] M.A. Elkestawy, S. Abdel kader, M.A. Amer, *Physica B* **405**, 619 (2010).
- [46] M.D. Migahed, M. Ishra, T. Fahmy, A. Barakat, *J. Phys. Chem. Solids* **65**, 1121 (2004).
- [47] Ş. Altındal, F. Parlaktürk, A. Tataroğlu, M.M. Bülbül, *J. Optoelectron. Adv. Mater.* **12**, 2139 (2010).
- [48] S.C. Watawe, B.D. Sarwade, S.S. Bellad, B.D. Sutar, B.K. Chougule, *J. Magn. Magn. Mater.* **214**, 55 (2000).
- [49] K. Prabakar, S.K. Narayandass and D. Mangalaraj, *Mater. Sci. Eng. B* **98**, 225 (2003).
- [50] C. Bharti, T.P. Sinha, *Solid State Sci.* **12**, 498 (2010).

Corresponding author: ademt@gazi.edu.tr